Am J Transl Res 2015;7(5):804-824
www.ajtr.org /ISSN:1943-8141/AJTR0007860

Original Article

Peripheral blood-derived endothelial progenitor cell therapy prevented deterioration of chronic kidney disease in rats

Tien-Hung Huang[1*], Yen-Ta Chen[2*], Pei-Hsun Sung[1], Hsin-Ju Chiang[3], Yung-Lung Chen[1], Han-Tan Chai[1], Sheng-Ying Chung[1], Tzu-Hsien Tsai[1], Chih-Chao Yang[4], Chih-Hung Chen[5], Yi-Ling Chen[1], Hsueh-Wen Chang[6], Cheuk-Kwan Sun[7], Hon-Kan Yip[1,8,9,10]

[1]Division of Cardiology, Department of Internal Medicine, Kaohsiung Chang Gung Memorial Hospital and Chang Gung University College of Medicine, Kaohsiung, 83301, Taiwan; [2]Division of Urology, Department of Surgery, Kaohsiung Chang Gung Memorial Hospital and Chang Gung University College of Medicine, Kaohsiung, 83301, Taiwan; [3]Department of Obstetrics and Gynecology, Kaohsiung Chang Gung Memorial Hospital and Chang Gung University College of Medicine, Kaohsiung, 83301, Taiwan; [4]Division of Nephrology, Department of Internal Medicine, Kaohsiung Chang Gung Memorial Hospital and Chang Gung University College of Medicine, Kaohsiung, 83301, Taiwan; [5]Division of General Medicine, Department of Internal Medicine, Kaohsiung Chang Gung Memorial Hospital and Chang Gung University College of Medicine, Kaohsiung, 83301, Taiwan; [6]Department of Biological Sciences, National Sun Yat-Sen University, Kaohsiung, 83301, Taiwan; [7]Department of Emergency Medicine, E-DA Hospital, I-Shou University, Kaohsiung, 82445, Taiwan; [8]Center for Shock Wave Medicine and Tissue Engineering, Kaohsiung Chang Gung Memorial Hospital and Chang Gung University College of Medicine, Kaohsiung, 83301, Taiwan; [9]Center for Translational Research in Biomedical Sciences, Kaohsiung Chang Gung Memorial Hospital and Chang Gung University College of Medicine, Kaohsiung, 83301, Taiwan; [10]Medical University Hospital, China Medical University, Taichung, 40402, Taiwan. [*]Equal contributors.

Received March 12, 2015; Accepted May 13, 2015; Epub May 15, 2015; Published May 30, 2015

Abstract: Background: This study tested the hypothesis that peripheral blood-derived endothelial progenitor cell (PBDEPC) therapy can impede the deterioration of chronic kidney disease (CKD) induced by 5/6 nephrectomy in rats. Methods and results: Adult-male rats (n = 30) were equally categorized into group 1 (sham control), group 2 (CKD only) and group 3 [CKD + PBDEPC (left intra-arterial (3.3×10^5) and penile vein (6.7×10^5) injections by day 14 after CKD induction]. By day 60, kidney blood flow (KBF) was significantly lower in group 2 than that in groups 1 and 3, and significantly lower in group 3 than that in group 1, whereas the levels of serum creatinine, and kidney injury score and size showed an opposite pattern compared to that of KBF among all groups (all $p < 0.001$). Protein expressions of apoptotic (caspase 3, PARP), inflammatory (TNF-α, MMP-9), oxidative-stress (oxidized protein, NOX-1), fibrotic (Smad3, TGF-β), and hypoxic/ischemic cell-stress (HIF-1α, p-Akt) biomarkers showed an opposite pattern, whereas angiogenesis at protein (eNOS, CD31) and cellular (CD31+, CXCR4+) levels showed an identical pattern compared to that of blood flow in all groups (all $p < 0.01$). Other pro-angiogenic biomarkers (SDF-1α, CXCR4, VEGF) at protein and cellular levels and antioxidants (HO-1+, NQO 1, GR+) at cellular level showed progressive significant increase from groups 1 to 3 (all $p < 0.001$). Conclusion: The results support that PBDEPC therapy effectively inhibits the propagation of CKD and the deterioration of renal function through enhancement of angiogenesis, blood flow, and anti-oxidative capacity as well as suppression of inflammation, oxidative stress, apoptosis, and fibrosis in a rodent model.

Keywords: Chronic kidney disease, 5/6 nephrectomy, apoptosis, inflammation, oxidative stress, angiogenesis

Introduction

Chronic kidney disease (CKD) of different etiologies is a growing epidemic that contributes to high morbidity and mortality in hospitalized patients [1-5]. Despite the state-of-the-art therapeutic modality and advanced pharmaceutical strategy, such as the uses of angiotensin converting enzyme inhibitor (ACEI), angiotensin II type I receptor blockade (ARB), and direct renin inhibitor (DRI), progressive deterioration of renal function is frequently observed, leading to the subsequent development of end-stage renal disease (ESRD) [6-8].

The aetiology of CKD is divergent and the mechanisms involved are complex. Endothelial cell dysfunction in the arterioles, followed by propagation and the development of obstructive atherosclerosis [9-12] has been implicated as one of the major aetiology in the pathogenesis of the disease. In particular, inflammatory reactions and oxidative stress have been reported to be the principal mechanisms involved [13-17]. Taken into account the variety of aetiologies and the complex mechanisms involved, satisfactory treatment of the disease with a single therapeutic strategy would be impossible. Therefore, finding a new therapeutic modality with relatively broad-spectrum effect for preservation of renal microvasculature and renal function is of utmost importance.

Growing experimental studies have demonstrated that stem cell therapy improves ischemia-related organ dysfunction [18-20]. Additionally, some clinical trials have shown that both endothelial progenitor cells (EPCs) and mesenchymal stem cells (MSCs) derived from bone marrow, peripheral blood, or adipose tissue significantly improve left ventricular function in the settings of acute myocardial infarction (AMI) and chronic ischemic heart disease [21-25]. The results of human studies [26, 27], including our recent trial [28], show that the number and function of EPCs decrease significantly in patients with CKD.

EPC therapy for ischemic organ dysfunction plays a crucial role in augmenting the expression of angiogenic factors, stimulating proliferation and maturation of new vessels in ischemic tissues, and promoting endothelial replacement after vascular injury [29-31].

In view of the fact that patients with CKD are usually refractory to traditional treatment strategies for complete restoration of renal function, cytotherapy may be a therapeutic alternative for these patients. Therefore, this study tested the hypothesis that peripheral blood-derived EPC (PBDEPC) therapy may impede the deterioration of CKD in a rat model.

Materials and methods

Ethics

All animal experimental procedures were approved by the Institute of Animal Care and Use Committee at Kaohsiung Chang Gung Memorial Hospital (Affidavit of Approval of Animal Use Protocol No. 2008121108) and performed in accordance with the Guide for the Care and Use of Laboratory Animals (NIH publication No. 85-23, National Academy Press, Washington, DC, USA, revised 1996).

Animal model of chronic kidney disease and animal grouping

Pathogen-free, adult male Sprague-Dawley (SD) rats (n = 48) weighing 320-350 g (Charles River Technology, BioLASCO Taiwan Co. Ltd., Taiwan) were randomized and equally divided into group 1 [sham controls (SC), n = 10), group 2 (CKD only, n = 10), and group 3 [CKD + PBDEPC (1.0×10^6)].

All animals were anesthetized by inhalational 2.0% isoflurane, placed supine on a warming pad at 37°C for midline laparotomies. Sham-operated rats (i.e., group 1) received laparotomy only, while CKD was induced in all animals in groups 2 and 3 by right nephrectomy plus arterial ligation of upper two-third (upper and middle poles) blood supplies of the left kidney [i.e., by leaving lower third (lower pole) kidney with normal blood supply]. Such a model allows preservation of limited amount of functioning renal parenchyma and offers simulation of CKD.

The dosage of EPC to be transfused in this CKD animal model was based on our previous reports [32-34] with some modifications.

Collection of peripheral blood, culture of endothelial progenitor cells, EPC labeling and treatment protocol

Rats in group 3 were anesthetized with inhalational 2.0% isoflurane at day 7 prior to CKD induction for the collection of 3 mL of peripheral blood from tail vein. The isolated mononuclear cells from peripheral blood were cultured in a 100 mm diameter dish with 10 mL DMEM culture medium containing 10% FBS. By 21-day culturing, 1.0×10^6 PBDEPC were obtained from each animal in group 3. Flow cytometric analysis was performed for identification of cellular characteristics (i.e., PBDEPC surface markers) after cell-labeling with appropriate antibodies on day 21 of cell cultivation prior to autologous implantation. On the other hand, rats in groups 1 and 2 were anesthetized with

inhalational 2.0% isoflurane and only received an identical procedure of peripheral blood sampling without further culture.

By day 14 after CKD induction, CM-DiI (Vybrant™ DiI cell-labeling solution, Molecular Probes, Inc.) (50 μg/ml) was added to the culture medium 30 minutes before cell transfusion for EPC labeling. The animals in each group were anesthetized with inhalational 2.0% isoflurane. Only laparotomy was done for each rat in groups 1 and 2. For those animals in group 3, autologous PBDEPC were carefully transfused through the left renal artery (3.3×10^5) and penile vein (6.7×10^5). After the procedure, the laparotomy wound was closed and the animals were allowed to recover from anaesthesia in a portable animal intensive care unit (ThermoCare®) for 24 hours.

Procedure and protocol of abdominal magnetic resonance imaging (MRI)

For abdominal MRI examination, the animals in each group were anesthetized with inhalational 2.0% isoflurane by day 60 prior to be sacrificed. Experiments were performed on a 9.4-T Bruker Biospec MRI system (Bruker Biospin, Ettlingen, Germany) equipped with a self-shielded magnet with a 20-cm clear bore and a BGA-12S gradient insert (12-cm inner diameter) that offered a maximal gradient strength of 675 mT m^{-1} and a minimum slew rate of 4673 T m^{-1} s^{-1}. The operational software of the scanner was Paravision (Bruker Biospin). During MRI signal acquisitions, animals were placed in supine position in a cradle made of Plexiglas. Body temperature was kept at 37°C using a heating pad. Following a short period of induction in a box, anesthesia was maintained with 3% isoflurane via a nose cone. All measurements were performed on spontaneously breathing animals; neither cardiac nor respiratory triggering was applied. A rat transmit-receive volume coil was used to performed MRI image. As a routine, high resolution T_2-weighted sagittal anatomical reference images were first recorded, using multislice turbo rapid acquisition with refocusing echoes (Turbo-RARE) sequence and the following parameters: field of view = 60.0 mm × 60.0 mm; matrix dimension = 256 × 256 pixels; spatial resolution = 46.8 μm × 46.8 μm; slice thickness = 1.5mm; echo time = 27.7 ms; repetition time = 3000 ms number of averages = 8; total acquisition time = 12 min. The sagittal and coronal anatomical imaging was performed on 10 adjacent slices sequentially per imaging session.

Abdominal ultrasonography for determining renal blood flow

For abdominal ultrasound examination, the animals in each group were anesthetized with inhalational 2.0% isoflurane by days 0, 14 and 60 prior to be sacrificed. After shaving the abdominal hair, abdominal ultrasound (Vevo 2100, Visual Sonics Inc., Toronto, Canada) was performed by an experienced technician blinded to the treatment protocol. The renal blood flow/velocity and color Doppler signals were carefully measured for three times in each rat. The parameters were averaged and entered into a computer for further analysis.

Assessment of blood urea nitrogen (BUN) and creatinine levels

To determine whether the animal model of CKD was successfully created, blood samples were serially collected before and after the CKD procedure (i.e., prior to and at day 14 and day 60) before being sacrificed. Concentrations of serum creatinine and blood urea nitrogen (BUN) were measured in duplicate using standard laboratory equipment. The mean intra-assay coefficient of variance for BUN and creatinine was less than 4.0%.

Determination of kidney parenchymal injury score

To elucidate the severity of kidney parenchymal injury after CKD induction, gross anatomical features of kidney in 4 animals of each group were estimated using the following scoring system:

1) Ratio of pelvis-calyces to medulla-cortex size score: score 0 = ratio < 0.7; score 1 = ratio ≥ 0.7-1.0; score 2 = ratio > 1. 2) Hilum & renal pelvis destructive score: 0 = no (i.e., intact); 1 = mild; 2 = moderate; 3 = severe. 3) Outer layer of medulla & inner layer of cortex necrosis score: 0 = no (i.e., intact); 1 = mild; 2 = moderate; 3 = severe.

Histopathology scoring of kidney injury at day 60 after CKD induction

The histopathology scoring of kidney injury was determined in a blinded fashion as we previ-

ously reported [32, 33]. Briefly, the left kidney specimens from all animals were fixed in 10% buffered formalin, embedded in paraffin, sectioned at 4 μm and stained (hematoxylin and eosin; H&E) for light microscopy. The score reflected the grading of tubular necrosis, loss of brush border, cast formation, and tubular dilatation in 10 randomly chosen, non-overlapping fields (200 ×) for each animal as follows: 0 (none), 1 (≤ 10%), 2 (11-25%), 3 (26-45%), 4 (46-75%), and 5 (≥ 76%).

Western blot analysis of right kidney specimens

The methods were previously detailed in our recent reports [32-34]. Primary antibodies against tumor necrosis factor (TNF)-α (1:1000, Cell Signaling), matrix metalloproteinase (MMP)-9 (1:1000, Millipore), NADPH oxidase (NOX)-1 (1:1500, Sigma), caspase 3 (1:1000, Cell Signaling), poly (ADP-ribose) polymerase (PARP) (1:1000, Cell Signaling), Bcl-2 (1:250, Abcam), endothelial nitric oxide synthase (eNOS) (1:1000, Abcam), CXCR4 (1:1000, Abcam), stromal cell-derived factor (SDF)-1α (1:1000, Cell Signaling), Smad3 (1:1000, Cell Signaling), Smad1/5 (1:1000, Cell Signaling), transforming growth factor (TGF)-β (1:500, Abcam), bone morphogenetic protein (BMP)-2 (1:500, Abcam), Bcl-2 (1:200, Abcam), hypoxia inducible factor (HIF)-1α (1:750, Abcam), phospho-Akt (1:1000, Cell Signaling) were used. Signals were detected with horseradish peroxidase (HRP)-conjugated goat anti-mouse, goat anti-rat, or goat anti-rabbit IgG.

The Oxyblot Oxidized Protein Detection Kit was purchased from Chemicon (S7150). The procedure was the same as we previously reported [32-34]. A standard control was loaded on each gel.

Immunoreactive bands were visualized by enhanced chemiluminescence (ECL; Amersham Biosciences), which was then exposed to Biomax L film (Kodak). For quantification, ECL signals were digitized using Labwork software (UVP). For oxyblot protein analysis, a standard control was loaded on each gel.

Immunohistochemical and immunofluorescent studies

The procedures and protocols for immunohistochemical (IHC) and immunofluorescent (IF) examinations were based on our recent studies [32-34]. Briefly, for IHC staining, rehydrated paraffin sections were first treated with 3% H_2O_2 for 30 minutes and incubated with Immuno-Block reagent (BioSB) for 30 minutes at room temperature. Sections were then incubated with primary antibodies specifically against glutathione reductase (GR; 1:100, Abcam) and NQO 1 (1:300, Abcam) at 4°C overnight. IF staining was performed for the examinations of CD31 (1:100, Bio SB), CXCR4 (1:100, Santa Cruz), heme oxygenase (HO-1) (1:250, Abcam), γ-H2AX (1:1000, Cell Signaling), respective primary antibody was used with irrelevant antibodies being used as controls. Three sections of kidney specimens were analyzed in each rat. For quantification, three randomly selected HPFs (× 200 for IHC and IF studies) were analyzed in each section. The mean number per HPF for each animal was then determined by summation of all numbers divided by 9. An IHC-based scoring system was adopted for semi-quantitative analyses of GR and NQO 1 in the kidneys as a percentage of positive cells in a blinded fashion (score of positively-stained cell for GR and NQO 1:0 = negative staining; 1 ≤ 15%; 2 = 15-25%; 3 = 25-50%; 4 = 50-75%; 5 ≥ 75%-100% per HPF).

Statistical analysis

Quantitative data are expressed as means ± SD. Statistical analyses were performed using SAS statistical software for Windows version 8.2 (SAS institute, Cary, NC) to conduct ANOVA followed by Bonferroni multiple-comparison post hoc test. A probability value < 0.05 was considered statistically significant.

Results

Flow cytometric results of peripheral blood-derived EPCs, blood urea nitrogen (BUN) and creatinine levels prior to and after CKD induction

By day 21 cell culture, the microscopic findings showed that the cells possessed cobblestone-like appearance, a typical picture of EPCs. Additionally, the flow cytometric analysis showed that the most popular EPCs were CD34+ cells.

By day 0 prior to CKD induction, the BUN and creatinine levels did not differ among the three groups. However, by day 14 after CKD induc-

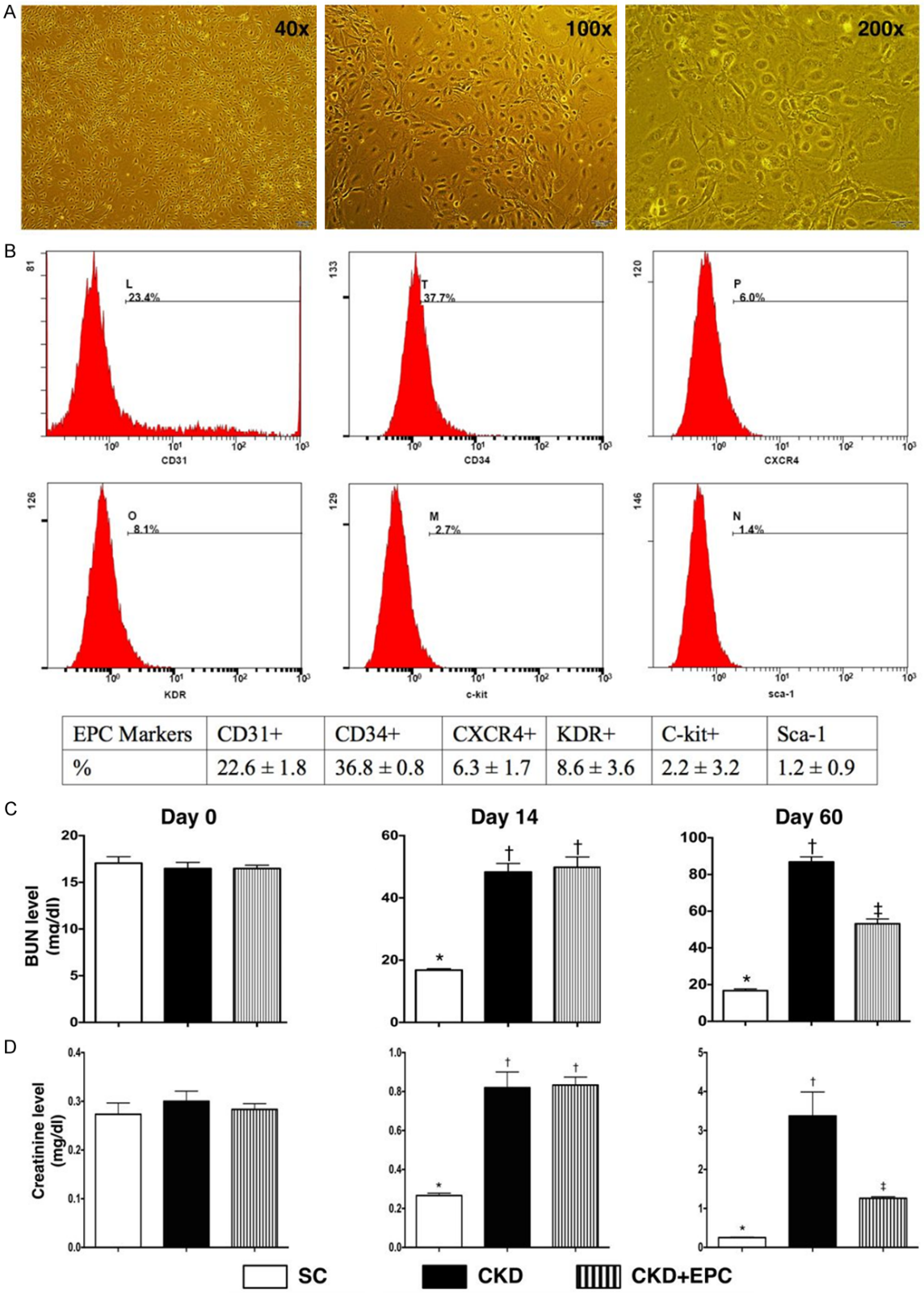

EPC Markers	CD31+	CD34+	CXCR4+	KDR+	C-kit+	Sca-1
%	22.6 ± 1.8	36.8 ± 0.8	6.3 ± 1.7	8.6 ± 3.6	2.2 ± 3.2	1.2 ± 0.9

Figure 1. Flow cytometric identification of peripheral blood-derived endothelial progenitor cells/stem cells and serial changes of circulating levels of blood urine nitrogen (BUN) and creatinine. A. By day 21 cell culturing, microscopic findings (40 ×, 100 ×, 200 ×) showed that the cells possessed cobblestone-like appearance, a typical picture of EPCs. B. Illustrating the flow cytometric results of surface markers of EPCs. The surface markers CD34+ cells was the most popular EPCs to be identified. C. The BUN level by day 14, * vs. †, $p < 0.0001$. The BUN level by day 60, *

vs. †, $p < 0.0001$. D. The creatinine level by day 14, * vs. †, $p < 0.001$. The creatinine level by day 60, * vs. other groups with different symbols (*, †, ‡), $p < 0.0001$. All statistical analyses were performed by one-way ANOVA, followed by Bonferroni multiple comparison post hoc test. Symbols (*, †, ‡) indicate significance (at 0.05 level). SC = sham control; CKD = chronic kidney disease; EPC = endothelial progenitor cell.

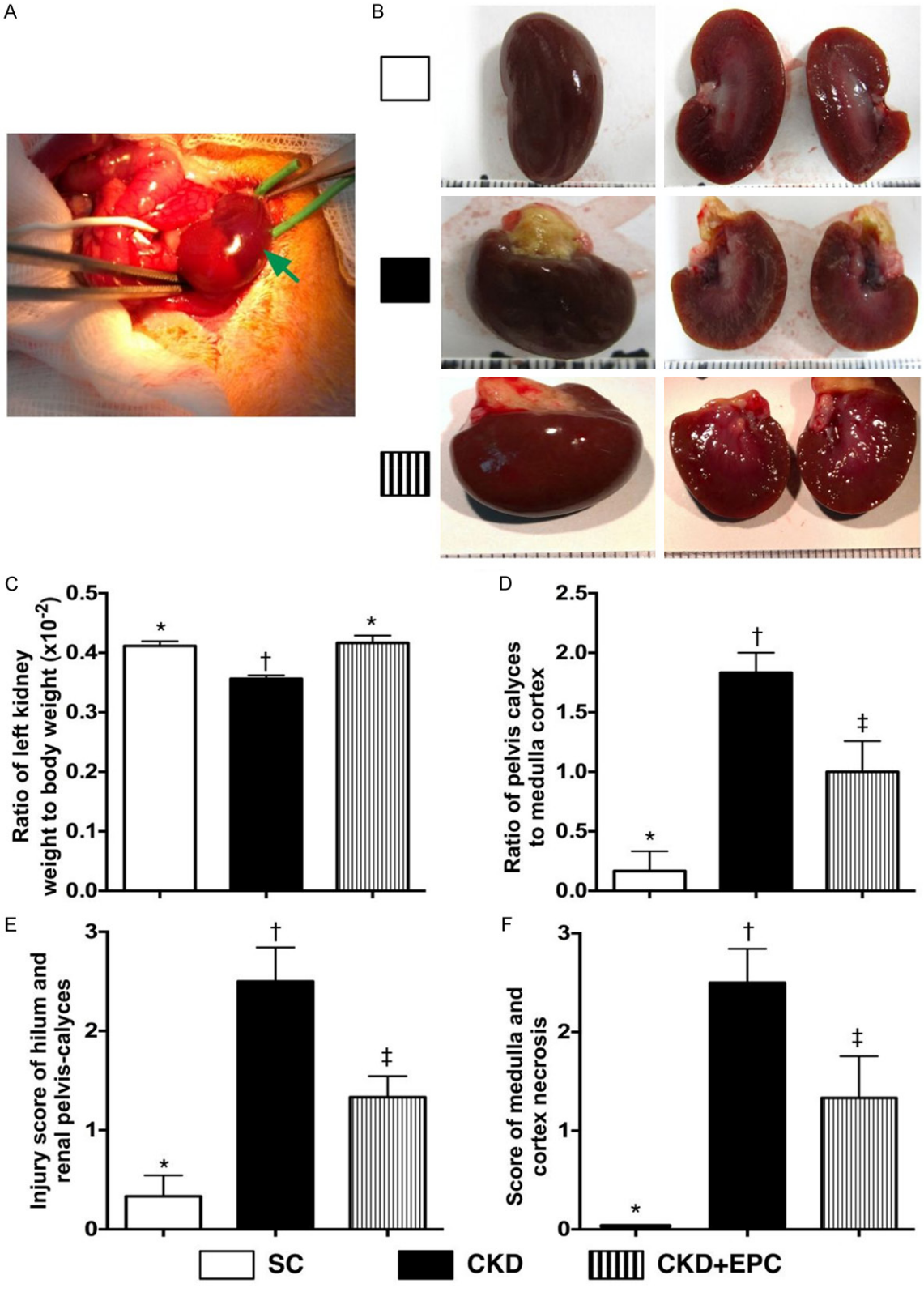

Figure 2. Grossly anatomical structure and measuring the kidney parenchymal injury score by day 60 after CKD induction (n = 10). A. Illustrating the operative finding of arterial ligation of upper two-third (i.e., upper and middle poles) of left kidney. The dark-color appearance (green arrow) was noted, an indicator of acute ischemia of left kidney. B. Illustrating the grossly anatomical finding of left kidney among three groups by day 60 after CKD induction. C. The ratio of left kidney to body weight (%),* vs. †, $p < 0.0001$. D. Ratio of pelvis calyces to medulla-cortex size, * vs. other groups with different symbols (*, †, ‡), $p < 0.0001$. E. Injury sore of hilum and pelvis calyces of left kidney, * vs. other groups with different symbols (*, †, ‡), * vs. †, $p < 0.0001$. F. Score of medulla and cortex necrosis of left kidney. All statistical analyses were performed by one-way ANOVA, followed by Bonferroni multiple comparison post hoc test. Symbols (*, †, ‡) indicate significance (at 0.05 level). SC = sham control; CKD = chronic kidney disease; EPC = endothelial progenitor cell.

tion, the serum level of BUN and creatinine were significantly higher in CKD and CDK-EPC than in SC, but there was no significant difference between the CKD and CKD-EPC groups. Additionally, by day 60 after CKD procedure, the serum BUN and creatinine levels were significantly higher in CKD and CKD-EPC than in those in SC and significantly higher in CKD than those in CKD-EPC (**Figure 1**). These findings imply that the CKD animal model was successfully created and that EPC therapy significantly prevented the deterioration of renal function in animals after CKD induction.

Assessment of anatomical structure and kidney parenchymal injury score

Grossly, the size of the kidney was notably larger in animals with untreated CKD than that in CKD-EPC and SC, and notably larger in the CKD-EPC group than that in SC. Consistently, the ratio of kidney to body weight was significantly lower in animals with untreated CKD than that in the CKD-EPC group and SC, but it showed no difference between CKD-EPC group and SC.

The kidney parenchymal injury scores, including: (1) ratio of pelvis-calyces to medulla-cortex size, (2) hilum and renal pelvis destructive feature, and (3) outer layer of medulla & inner layer of cortex necrosis, were significantly higher in CKD group than in CKD-EPC and SC, and significantly higher in the CKD-EPC than in the SC (**Figure 2**).

Abdominal MRI and ultrasound findings of the kidneys among the three groups

In the present study, abdominal MRI was utilized to identify the anatomical structure of cortex and medulla of the kidney. The contour of the kidney (i.e., cortex and medulla) was intact in SC animals. By contrast, the cortex of left kidney was notably thinner in the CKD-EPC group and even more remarkable in animals with untreated CKD by day 60 after CKD induction. In addition, the medulla was found to be intact in SC, partially preserved in the CKD-EPC group, and lost in most of the animals with untreated CKD. More over, the cavity of left calyx was intact in SC, significantly enlarger in CKD-EPC group and more remarkable in animals with untreated CKD.

Renal ultrasonography showed that, by day 60 after CKD procedure, the kidney size was significantly increased in animals with untreated CKD than that in the CKD-EPC group and SC, and significantly reduced in the CKD-EPC group than that in SC. Additionally, the sizes of cortex and medulla showed an opposite pattern of kidney size among the four groups. On the other hand, renal blood flow was significantly reduced in animals with untreated CKD than that in the CKD-EPC group and SC, and significantly reduced in the CKD-EPC group than that in SC (**Figure 3**). These findings suggest that EPC therapy preserves integrity of kidney architecture and renal blood flow after CKD induction.

Histological damage of kidney parenchyma by day 60 after CKD induction

H&E staining of left kidney sections revealed that kidney injury score was significantly higher in animals with untreated CKD than that in the CKD-EPC group and SC, and significantly higher in the CKD-EPC group than that in SC (**Figure 4**). Accordingly, the pathological finding suggests that EPC therapy protects the kidney against CKD-induced histological damage.

Protein expressions of apoptosis and fibrosis in kidney parenchyma by day 60 after CKD induction

The protein expressions of cleaved caspase 3 and cleaved PARP, two indices of apoptosis, were significantly higher in animals with

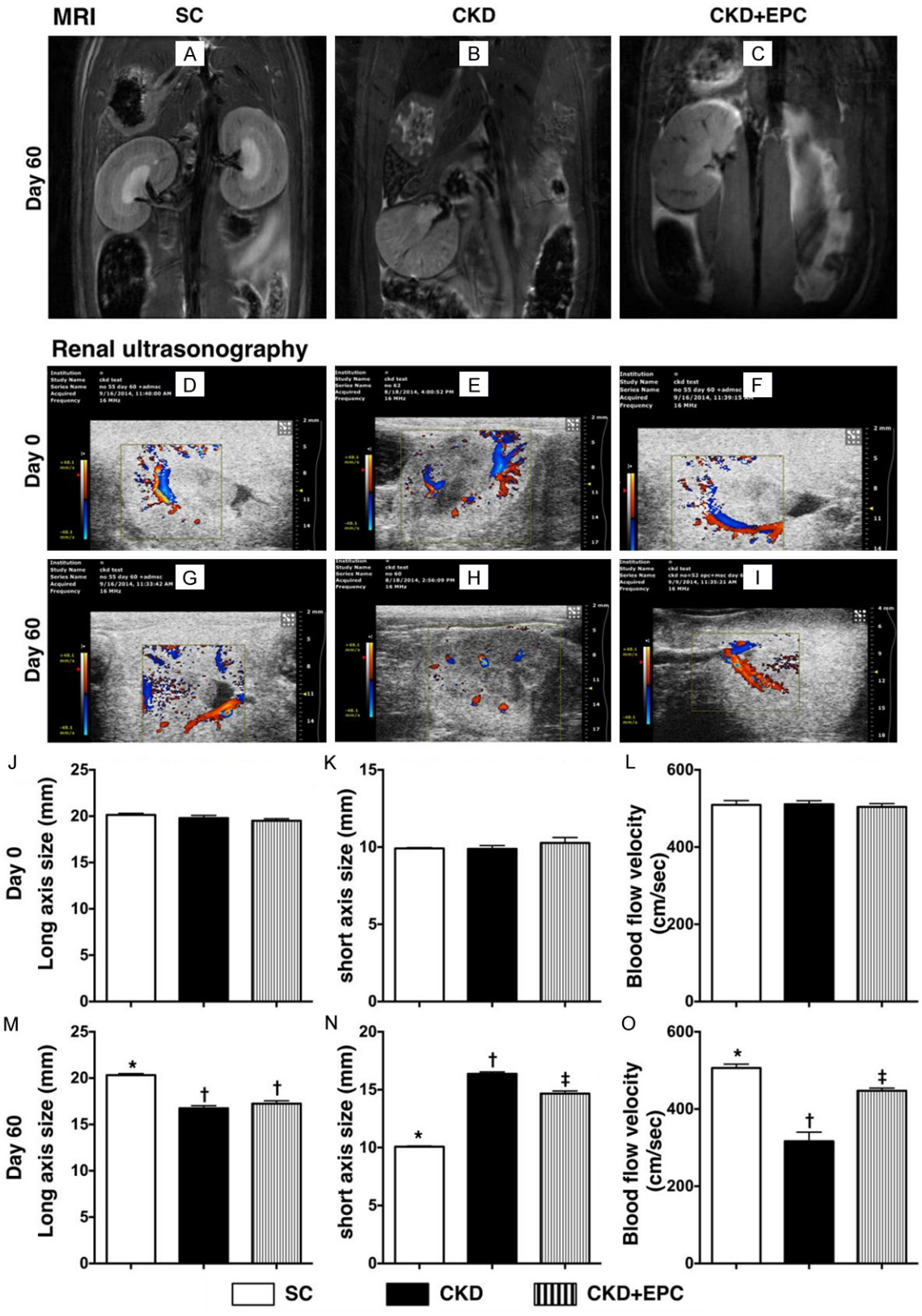

Figure 3. Imaging findings of left kidneys among the three groups by day 60 after CKD induction (n = 10). A-C. Illustrating the magnetic resonance imaging (MRI) finding (coronal section) of left renal parenchymal structure. The MRI results showed that gross anatomical feature (i.e. bean shaped) morphological feature of cross section (i.e., the pelvis calyces, medulla and cortex) of kidney were lost in CKD, partially preserved in CKD-EPC and intact in SC.

D-F. Illustrating the abdominal ultrasound findings of blood flow in the kidney by day 0 prior to CKD induction. The blood flood was homogeneous and did not differ among the three groups. G-I. Illustrating the abdominal ultrasound findings of blood flow in the kidney by day 60 after CKD induction. The blood flood was remarkably lower in CKD (H) group than the other groups. J-L. By day 0, the long axis size (J), short axis size (K) and the blood flow velocity of left kidney did not differ among the three groups. M. The analytical result of long axis size of left kidney by day 60 after CKD induction, * vs. †, $p < 0.001$. N. Analytical result of short axis size of left kidney by day 60 after CKD induction, * vs. other groups with different symbols (*, †, ‡), * vs. †, $p < 0.0001$. O. The analytic results of blood flow velocity of left kidney by day 60 after CKD induction, * vs. other groups with different symbols (*, †, ‡), * vs. †, $p < 0.0001$. All statistical analyses were performed by one-way ANOVA, followed by Bonferroni multiple comparison post hoc test. Symbols (*, †, ‡) indicate significance (at 0.05 level). SC = sham control; CKD = chronic kidney disease; EPC = endothelial progenitor cell.

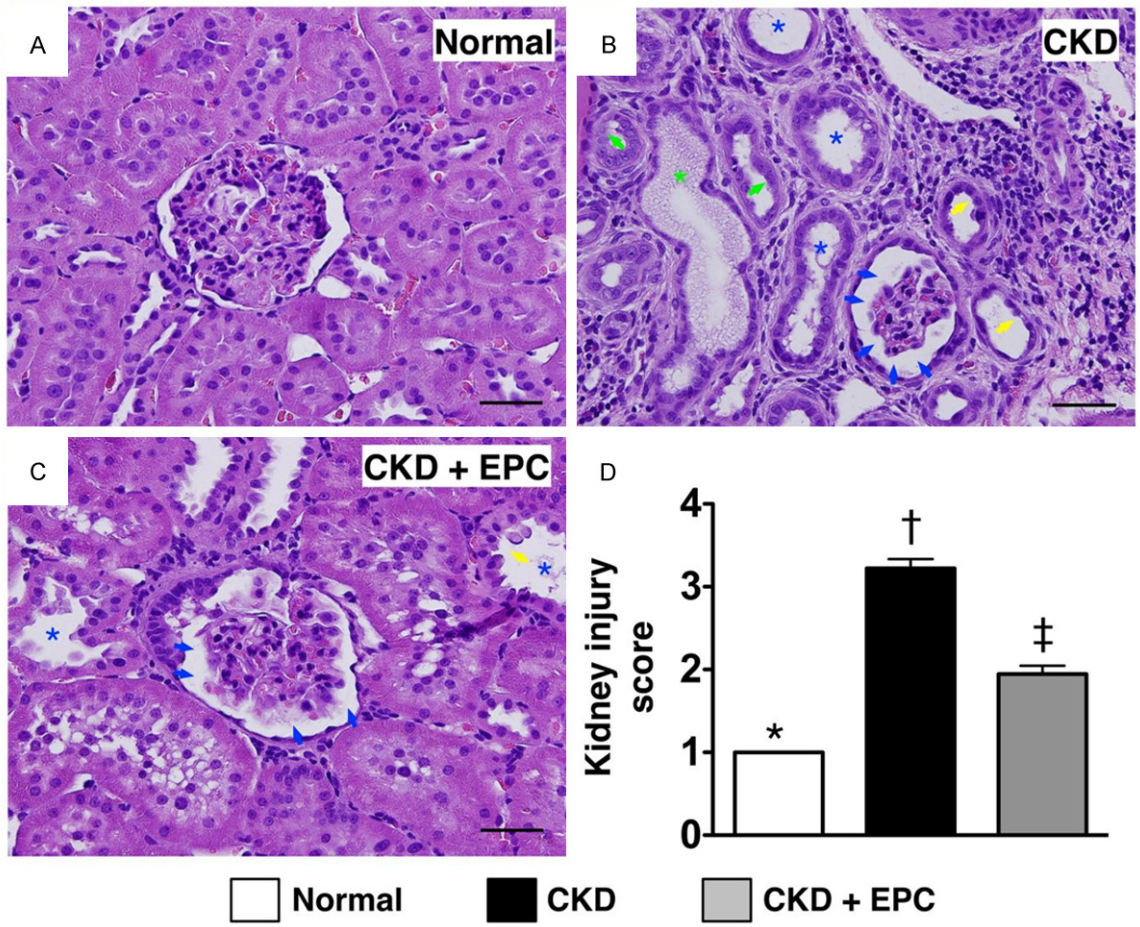

Figure 4. Histopathological findings of kidney injury by day 60 after CKD induction (n = 10). A to C. H. & E. stain (200 ×) demonstrating significantly higher degree of loss of brush border in renal tubules (yellow arrows), cast formation (green asterisk), tubular dilatation (blue asterisk) tubular necrosis (green arrows), and dilatation of Bowman's capsule (blue arrows) in CKD group than in other groups. D. * vs. other groups with different symbols (*, †, ‡), * vs. †, $p < 0.0001$. All statistical analyses were performed by one-way ANOVA, followed by Bonferroni multiple comparison post hoc test. Symbols (*, †, ‡) indicate significance (at 0.05 level). Scale bars in right lower corner represent 50 μm. SC = sham control; CKD = chronic kidney disease; EPC = endothelial progenitor cell.

untreated CKD than those in the CKD-EPC treatment group and SC, and significantly higher in the CKD-EPC group than that in SC. Moreover, Smad3 and TGF-β, two indicators of fibrosis, exhibited an identical pattern compared to that of apoptotic markers among the three groups. Conversely, the protein expressions of Bcl-2, an indicator of anti-apoptosis, and Smad1/5 and BMP-2, two indicators of anti-fibrosis, showed an opposite pattern compared to that of apoptosis among three groups (**Figure 5**).

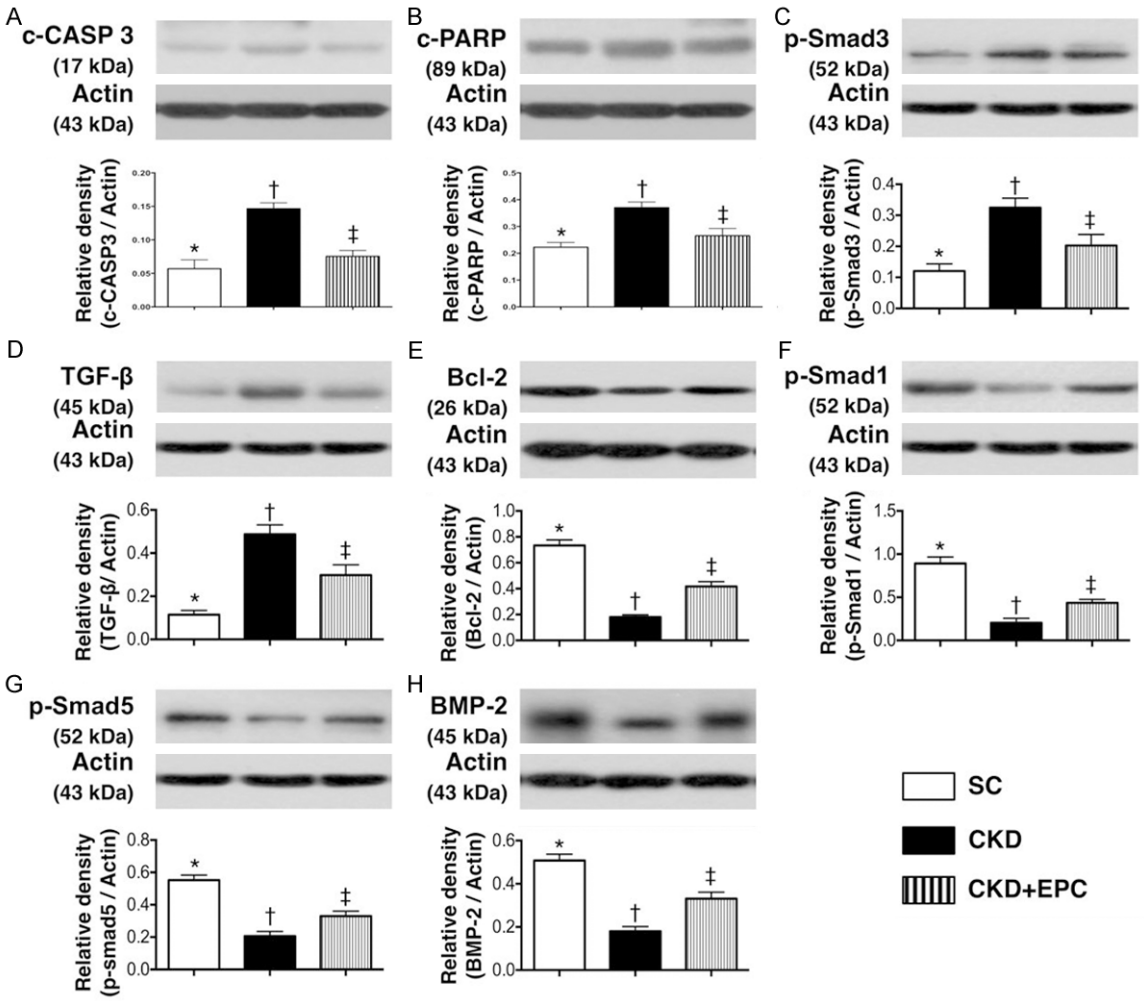

Figure 5. Protein expressions of apoptosis and fibrosis in kidney parenchyma by day 60 after CKD Induction (n = 10). A. Protein expression of cleaved (c) caspase 3, * vs. other groups with different symbols (*, †, ‡), * vs. †, $p < 0.001$. B. Protein expression of cleaved (c) poly (ADP-ribose) polymerase (PARP), * vs. other groups with different symbols (*, †, ‡), * vs. †, $p < 0.01$. C. Protein expression of Smad3, * vs. other groups with different symbols (*, †, ‡), * vs. †, $p < 0.001$. D. Protein expression of transforming growth factor (TGF)-β, * vs. other groups with different symbols (*, †, ‡), * vs. †, $p < 0.001$. E. Protein expression of Bcl-2, * vs. other groups with different symbols (*, †, ‡), * vs. †, $p < 0.001$. F, G. Protein expression Smad1/5, * vs. other groups with different symbols (*, †, ‡), * vs. †, $p < 0.001$. H. Protein expression of bone morphogenetic protein (BMP)-2, * vs. other groups with different symbols (*, †, ‡), * vs. †, $p < 0.001$. All statistical analyses were performed by one-way ANOVA, followed by Bonferroni multiple comparison post hoc test. Symbols (*, †, ‡) indicate significance (at 0.05 level). Scale bars in right lower corner represent 50 μm. SC = sham control; CKD = chronic kidney disease; EPC = endothelial progenitor cell.

Protein expressions of inflammatory and oxidative stress biomarkers in kidney parenchyma by day 60 after CKD induction

The protein expressions of TNF-α and MMP-9, two indicators of inflammation, were significantly higher in rats with untreated CKD than those in the CKD-EPC group and SC, and significantly higher in the CKD-EPC group than that in SC. Similarly, NOX-1, an indicator of reactive oxygen species (ROS), and oxidized protein, an indicator of oxidative stress, displayed an identical pattern compared to that of inflammatory biomarkers among the five groups (**Figure 6**).

Protein expressions of pro-angiogenic factors in kidney parenchyma by day 60 after CKD induction

The protein expression of VEGF, CXCR4, and SDF-1α, three indices of angiogenesis, showed a significant progressive increase from SC to

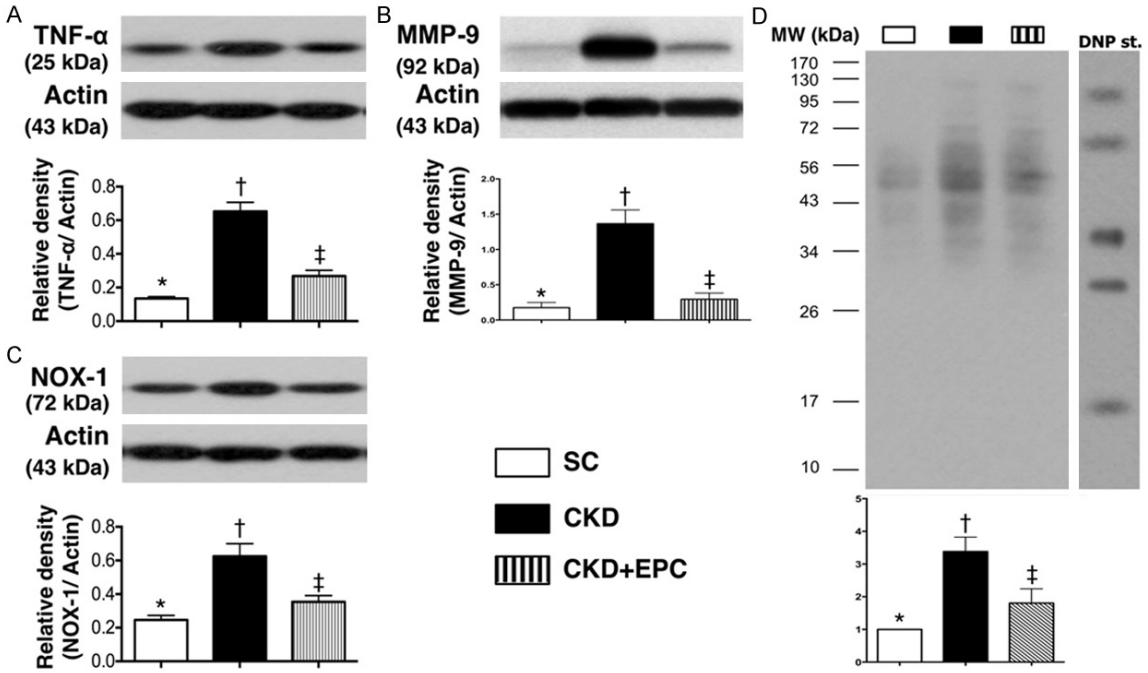

Figure 6. Protein expressions of inflammatory and oxidative stress biomarkers in kidney parenchyma by day 60 after CKD induction (n = 10). A. Protein expression of tumor necrosis factor (TNF)-α, * vs. other groups with different symbols (*, †, ‡), * vs. †, $p < 0.001$. B. Protein expression of matrix metalloproteinase (MMP-9), * vs. other groups with different symbols (*, †, ‡), * vs. †, $p < 0.001$. C. Protein expression of NOX-1, * vs. other groups with different symbols (*, †, ‡), * vs. †, $p < 0.001$. D. The oxidized protein expression, * vs. other groups with different symbols (*, †, ‡, §), $p < 0.0001$. (Note: left and right lanes shown on the upper panel represent protein molecular weight marker and control oxidized molecular protein standard, respectively). M.W = molecular weight; DNP = 1-3 dinitrophenylhydrazone. All statistical analyses were performed by one-way ANOVA, followed by Bonferroni multiple comparison post hoc test. Symbols (*, †, ‡) indicate significance (at 0.05 level). Scale bars in right lower corner represent 50 μm. SC = sham control; CKD = chronic kidney disease; EPC = endothelial progenitor cell.

the CKD-EPC group. In addition, the protein expression of eNOS and CD31, another two indicators of angiogenesis, was significantly higher in SC than in animals with untreated CKD and those in the CKD-EPC group, and significantly higher in the CKD-EPC group than that in animals with untreated CKD. On the other hand, the protein expressions of HIF-1α and p-Akt, two indicators of cellular hypoxic/ischemic stress, were significantly higher in animals with untreated CKD than those in the CKD-EPC group and SC, and significantly higher in the CKD-EPC group than those in SC (**Figure 7**).

Expressions of anti-oxidants and DNA damage marker in renal parenchyma by day 60 after CKD induction

IHC staining for cells positive for GR and NQO 1, two indices of anti-oxidants (i.e. scavengers), showed that the number of cells positive for the two biomarkers was significantly higher in the CKD-EPC treatment group than that in animals with untreated CKD and in SC, and significantly higher in animals with untreated CKD than those in SC (**Figure 8**). Similarly, IF staining demonstrated that the pattern of changes in the number of cells positive for HO-1 (i.e., another index of anti-oxidant) in the three groups was identical to that of changes in the number of cells positive for GR and NQO 1 (**Figure 9**). These findings imply that kidney ischemia resulted from CKD would elicit an up-regulation of intrinsic anti-oxidants in kidney, thereby protecting kidney parenchyma from damage. Also, EPC therapy offered the protection against 5/6 nethrectomy-induced kidney injury through up-regulation of anti-oxidants. On the other hand, the number of cells positive for γ-H2AX, an indicator of DNA damage, was significantly higher in animals with untreated CKD than that in the CKD-EPC group and SC,

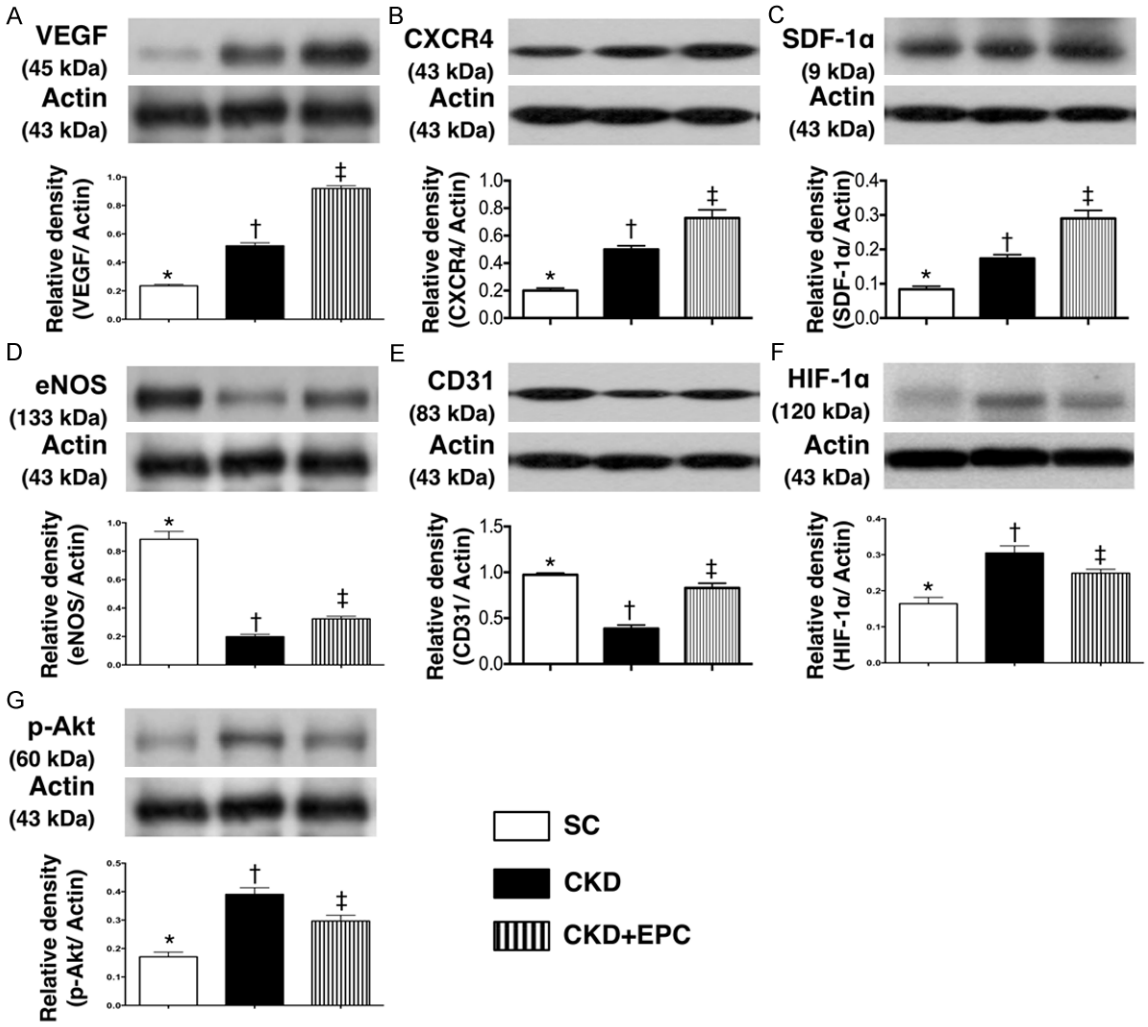

Figure 7. Protein Expressions of Pro-angiogenic Factors in Kidney Parenchyma by Day 60 after CKD Induction (n = 10). A. Protein expression of vascular endothelial growth factor (VEGF), * vs. other groups with different symbols (*, †, ‡), * vs. †, $p < 0.0001$. B. Protein expression of CXCR4, * vs. other groups with different symbols (*, †, ‡), * vs. †, $p < 0.0001$. C. Protein expression of stromal cell-derived factor (SDF)-1α, * vs. other groups with different symbols (*, †, ‡), * vs. †, $p < 0.0001$. D. Protein expression of eNOS, * vs. other groups with different symbols (*, †, ‡), * vs. †, $p < 0.0001$. E. Protein expression of CD31, * vs. other groups with different symbols (*, †, ‡), * vs. †, $p < 0.01$. F. Protein expression of hypoxic inducible factor (HIF)-1α, * vs. other groups with different symbols (*, †, ‡), * vs. †, $p < 0.01$. G. Protein expression of phosphoryated (p)-Akt, * vs. other groups with different symbols (*, †, ‡), * vs. †, $p < 0.0001$. All statistical analyses were performed by one-way ANOVA, followed by Bonferroni multiple comparison post hoc test. Symbols (*, †, ‡) indicate significance (at 0.05 level). Scale bars in right lower corner represent 50 μm. SC = sham control; CKD = chronic kidney disease; EPC = endothelial progenitor cell.

and significantly higher in the CKD-EPC group than that in SC (**Figure 9**).

Identification of EPC engrafted in renal parenchyma

Under fluorescent microscope, numerous CM-Dil-positive EPCs were identified in renal parenchyma of CKD-EPC animals. Interestingly, some of these EPCs were found to engraft to interstitial, peri-tubular and glomerular areas of kidney. In addition, some cells positively-stained for CD31, an indicator of endothelial-type phenotypes, and some cells positively-stained for CXCR4, an indicator of EPC, was found to be located in interstitial and peri-tubular regions and some of them were shown to engraft to the epithelial tubular and glomerular

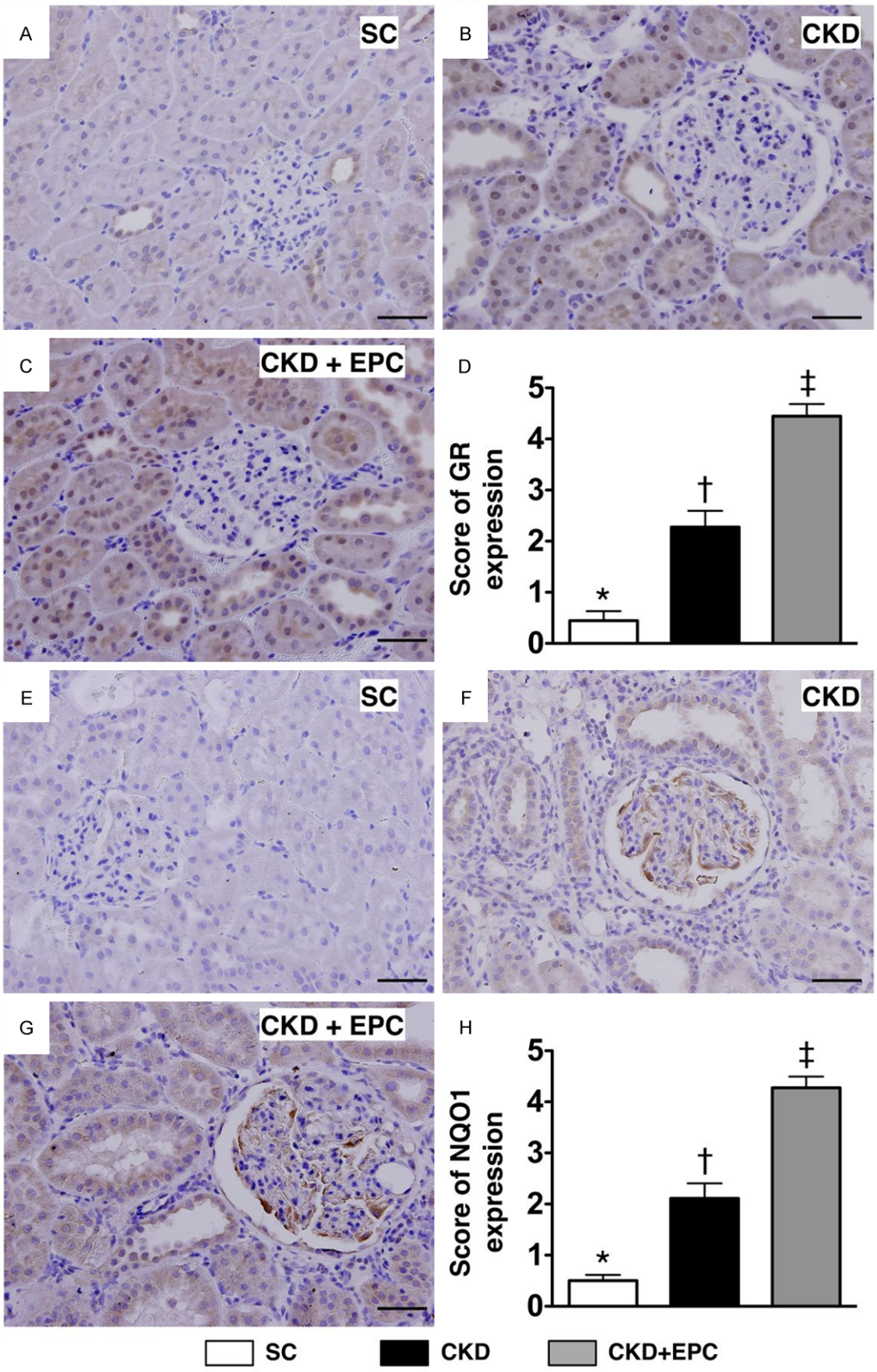
A
SC
B
CKD
C
CKD + EPC
D
Score of GR expression
0
1
2
3
4
5
*
†
‡
E
SC
F
CKD
G
CKD + EPC
H
Score of NQO1 expression
0
1
2
3
4
5
*
†
‡
SC
CKD
CKD+EPC

Figure 8. Immunohistochemical (IHC) staining for quantifying the antioxidants of glutathione reductase (GR) and NQO 1 in kidney parenchyma at day 60 after CKD induction (n = 10). A to C. IHC microscopic (200 ×) findings of number of GR+ cells (gray color) in three groups of animals. D. Analytical results, * vs. other groups with different symbols (*, †, ‡), * vs. †, $p < 0.0001$. Scale bars in right lower corner represent 50 μm. E to G. Microscopic (200 ×) IHC staining for identifying the number of NAD(P)H quinone oxidoreductase (NQO) 1+ cells (gray color) in all groups. H. Analytical results, * vs. other groups with different symbols, $p < 0.0001$. Scale bars in right lower corner represent 50 μm. All statistical analyses were performed by one-way ANOVA, followed by Bonferroni multiple comparison post hoc test. Symbols (*, †, ‡) indicate significance (at 0.05 level). Scale bars in right lower corner represent 50 μm. SC = sham control; CKD = chronic kidney disease; EPC = endothelial progenitor cell.

area (**Figure 10**). These findings suggest that angiogenesis occurred in peri-tubular and glomerular regions for possible tubular and glomerular repair and regeneration after EPC transplantation.

Discussion

This study, which investigated the therapeutic effect of EPC against the deterioration of kidney function from 5/6 nephrectomy-induced CKD, produced several striking implications. First, 5/6 nephrectomy successfully provided a consistent CKD animal model for investigating the therapeutic potential of EPC in the setting of CKD. Second, the integrity of left kidney architecture was substantially protected after EPC therapy in animals with CKD. Third, renal function and the blood flow in the left kidney were remarkably preserved after EPC treatment in animals after CKD induction. Finally, EPC treatment markedly enhanced angiogenesis and production of antioxidants, and notably suppressed inflammation, oxidative stress, apoptosis, and fibrosis.

Preclinical successful experience encourages the translational research in clinical application of EPCs for CKD patients

Surprisingly, while clinical trials have shown that both EPC and MSC therapies significantly improve ischemia-related organ dysfunction [21-25], the potential therapeutic impact of EPC treatment on kidney function in patient with CKD has not been reported. Besides, only a few experimental studies [35, 36] have reported the benefit of EPC treatment on the preservation of renal function in the setting of CKD. Therefore, prior to the application of EPC in the clinical setting of CKD, more experimental studies are warranted to elucidate the mechanisms involved and to prove the true clinical benefit of EPC treatment on restoring renal function.

An important finding of the present study is that, up to the end of study period (i.e., by day 60 after CKD induction), end-stage of renal disease was noted in animals with untreated CKD. Of importance is the fact that renal function (i.e., circulating level of creatinine) at day 60 was significantly preserved to a degree comparable to that of day 14 after CKD procedure in animals with CKD after EPC treatment. Two previous experimental studies using large (i.e., pig) [35] or small (i.e., mouse) [36] animal models of CKD demonstrated that kidney function was significantly restored after receiving EPC derived either from peripheral blood [35] or bone marrow [36]. Accordingly, our findings, in addition to being consistent with those of previous studies [35, 36], encourage the conduction of a prospective clinical trial to investigate the therapeutic potential of autologous EPC transfusion for patients with CKD who failed to respond to traditional therapy.

Grossly anatomical-pathological findings, abdominal MRI examination and ultrasound results supported the effects of EPC therapy preserved the renal architecture

The principal finding in the present study was that the anatomical findings revealed that kidney parenchymal injury scores were remarkably higher in CKD animals as compared with those of controls. However, these injury score were markedly reduced in those of CKD animals after receiving EPC therapy. Interestingly, the abdominal MRI finding showed that the integrities of both medulla and cortex of the left kidney were remarkably disrupted in animals with untreated CKD compared to those in the sham controls. However, the integrity of the left kidney architecture was notably preserved in animals with CKD after EPC treatment. Additionally, another interesting finding in the present study is that abdominal sonography showed that kidney size of short axis was remarkably reduced and the integrity of both cortex and medulla

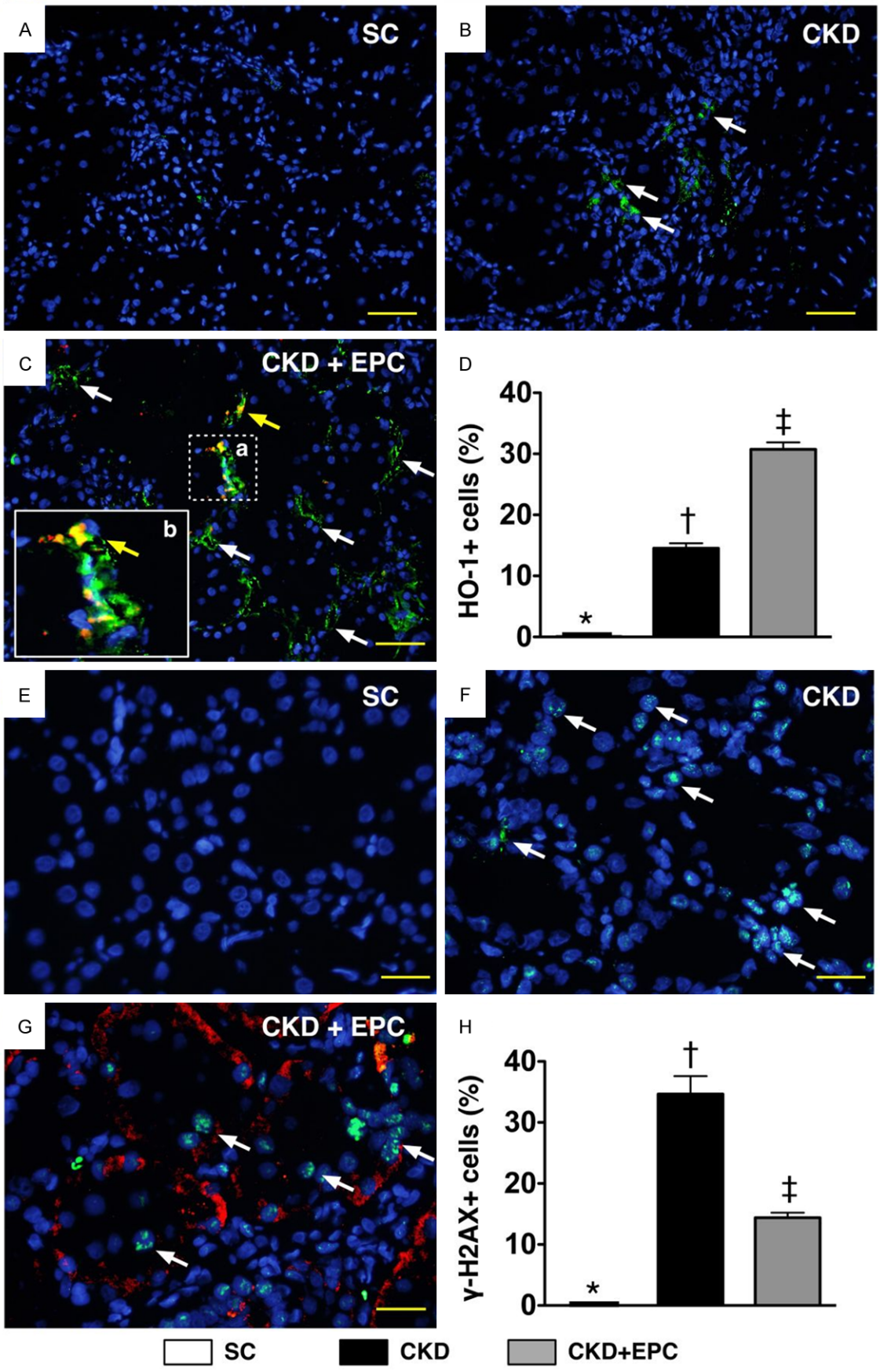
A
SC
B
CKD
C
CKD + EPC
a
b
D
HO-1+ cells (%)
40
30
20
10
0
*
†
‡
E
SC
F
CKD
G
CKD + EPC
H
γ-H2AX+ cells (%)
40
30
20
10
0
*
†
‡
SC
CKD
CKD+EPC

Figure 9. Immunofluorescent (IF) staining for Identification of cellular expressions of heme oxygense (HO)-1+ cells and γ-H2AX+ cells in Renal Parenchyma by Day 60 after CKD Induction (n = 10). A to C. IF microscopic finding (200 ×) for identification of number of HO-1+ cells (white arrows). Some mixed color of red-yellowish cells (yellow arrows) with positively double stain (i.e., merged CM-DiI dye + HO-1 staining) were present, suggesting some transfused EPCs migrated to the kidney and developed into positively stained HO-1+ cells. The magnified (b) picture (solid square) from small dot-line square (a) showed typical feature of double stain HO-1+ cells. DAPI counter-staining for nuclei (blue) D. Analytical results, * vs. other groups with different symbols, $p < 0.0001$. Scale bars in right lower corner represent 50 μm. E to G. IF microscopic (400 ×) finding for identification of number of γ-H2AX+ cells (white arrows). Some transfused EPCs (yellow arrows) were identified to be present in the kidney parenchyma. DAPI counter-staining for nuclei (blue). H. Analytical results, * vs. other groups with different symbols, $p < 0.0001$. Scale bars in right lower corner represent 20 μm. All statistical analyses were performed by one-way ANOVA, followed by Bonferroni multiple comparison post hoc test. Symbols (*, †, ‡) indicate significance (at 0.05 level). Scale bars in right lower corner represent 50 μm. SC = sham control; CKD = chronic kidney disease; EPC = endothelial progenitor cell.

were notably preserved in CKD animals after EPC treatment than in those of CKD animals.

Importantly, a remarkable preservation of blood flow to the left kidney in animals with CKD after EPC treatment compared to the significantly reduced renal blood flow in animals with untreated CKD was observed in the present study. In this way, the MRI and ultrasound findings support the anatomical findings in the present study.

EPC therapy markedly reversed the molecular-cellular perturbations in CKD animals

Of importance was that as compared with the sham controls, H&E staining showed a marked increase in kidney injury score in animals with untreated CKD. On the other hand, the score was substantially reduced in animals with CKD treated with EPCs. These findings could explain the preservation of renal function in animals with CKD after EPC treatment.

Intriguingly, further analysis demonstrated that the expressions of pro-angiogenic biomarkers were significantly higher in the CKD-EPC group than in those animals with untreated CKD at both cellular and protein levels. This finding could, at least in part, explain the preservation of the renal microvasculature, the restoration of the renal blood flow, and ultimately the maintenance of renal function after EPC treatment in the present study.

An essential finding in the present study is that, as compared with the sham controls, the expressions of inflammatory, apoptotic, fibrotic, oxidative-stress, and DNA damage biomarkers in the left kidney were substantially augmented, whereas those of anti-fibrotic biomarkers were remarkably reduced in animals with untreated CKD. By contrast, these cellular and molecular perturbations as well as the expression of anti-oxidant biomarkers were markedly reversed in animals with CKD after EPC therapy. Intriguingly, previous studies have identified inflammatory reaction and oxidative stress as the principal contributors to renal injuries in the setting of CKD [13, 15-17, 33]. Moreover, our findings are also consistent with those of previous experimental studies that showed significant associations among the enhancement of fibrosis, apoptosis, DNA and organ damage in the setting of ischemia-reperfusion injury [16-18, 32-34], shedding light on the mechanisms underlying the observed preservation of renal structural and functional integrity in animals with CKD after EPC treatment.

Study limitations

This study has limitations. First, this study did not investigate the optimal dosage of EPC for maximal benefit in terms of renal function preservation in the present experimental setting. Second, despite the extensive experimental work in the current study, the exact mechanisms underlying the improvement of renal function remains uncertain. The proposed mechanisms for the observed protection offered by EPC in a rodent model of CKD based on our findings have been summarized in **Figure 11**.

In conclusion, the results of the present study highlight the effectiveness of EPC treatment in restoring renal function and preservation of the integrity of renal parenchyma in an experimental setting of CKD.

Acknowledgements

This study was supported by a program grant from Chang Gung Memorial Hospital, Chang

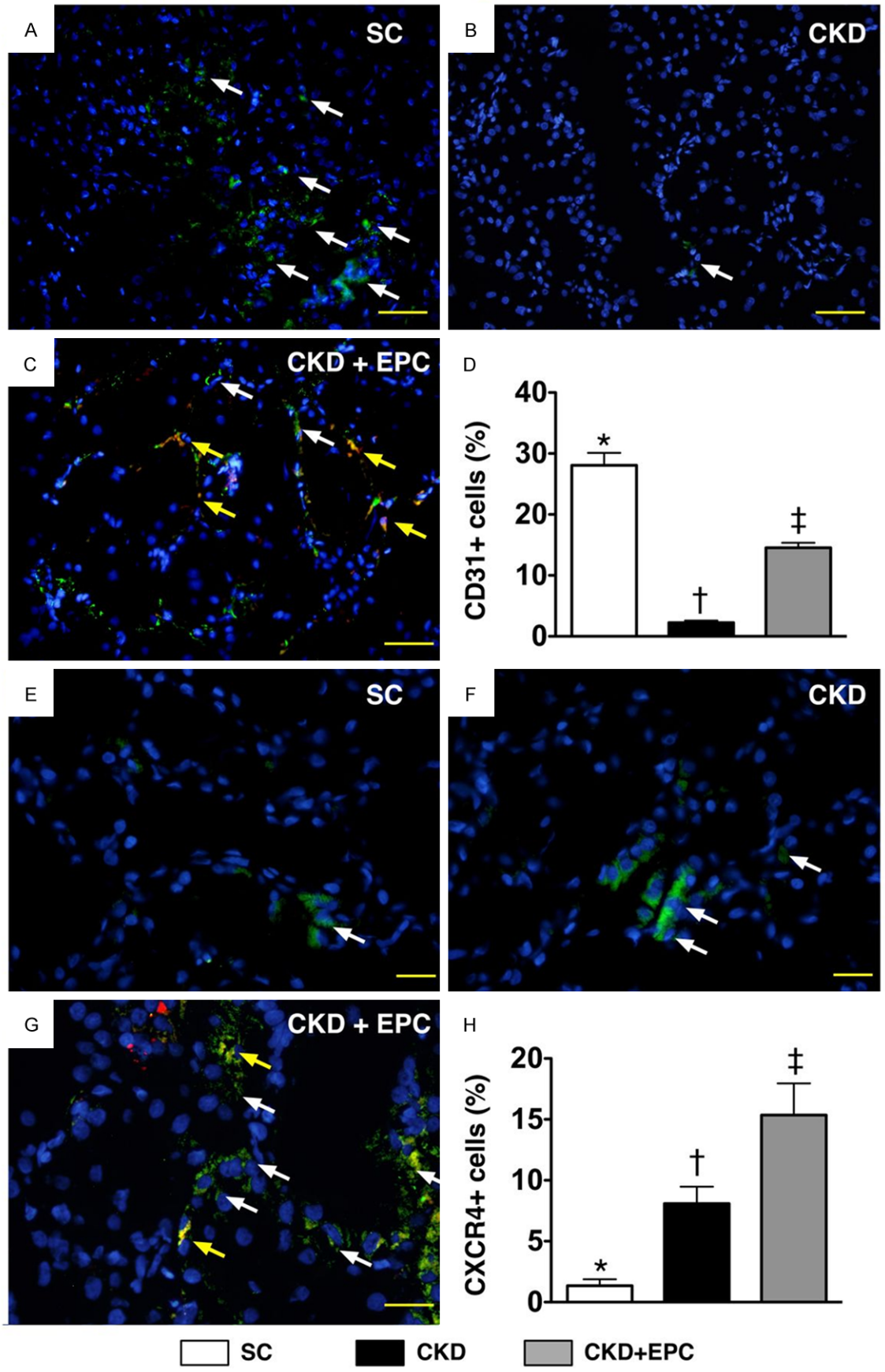
A
SC
B
CKD
C
CKD + EPC
D
CD31+ cells (%)
40
30
20
10
0
*
†
‡
E
SC
F
CKD
G
CKD + EPC
H
CXCR4+ cells (%)
20
15
10
5
0
*
†
‡
SC
CKD
CKD+EPC

Figure 10. Immunofluorescent (IF) stains of presence of CD31+ and CXCR4+ cells in renal parenchyma at day 60 after CKD induction (n = 8). A to C. IF staining (200x) of CD31+ cells (white) in renal parenchyma. Merged image from double staining (Dil dye + CD31) (C) showing cellular elements of mixed red and yellow (red arrows) under higher magnifications [(b) being magnified image of (a)], indicating transplanted numerous doubly-stained cells (CD31+) in peri-tubular and interstitial areas. DAPI counter-staining for nuclei (blue). Scale bars at right lower corner represent 50 μm. D. * vs. other groups with different symbols (*, †, ‡), $p < 0.0001$. E to G. IF staining (400 ×) of CXCR+ cells (white) in renal parenchyma. Merged image from double staining (Dil dye + CXCR4) showing cellular elements of mixed red and yellow (red arrows) under higher magnifications [(c) being magnified images of (d)], indicating implanted doubly-stained cells (CDCR4+) in peri-tubular and interstitial areas. DAPI counter-staining for nuclei (blue). Scale bars at right lower corner represent 20 μm. H. * vs. other groups with different symbols (*, †, ‡), $p < 0.0001$. All statistical analyses were performed by one-way ANOVA, followed by Bonferroni multiple comparison post hoc test. Symbols (*, †, ‡) indicate significance (at 0.05 level). Scale bars in right lower corner represent 50 μm. SC = sham control; CKD = chronic kidney disease; EPC = endothelial progenitor cell.

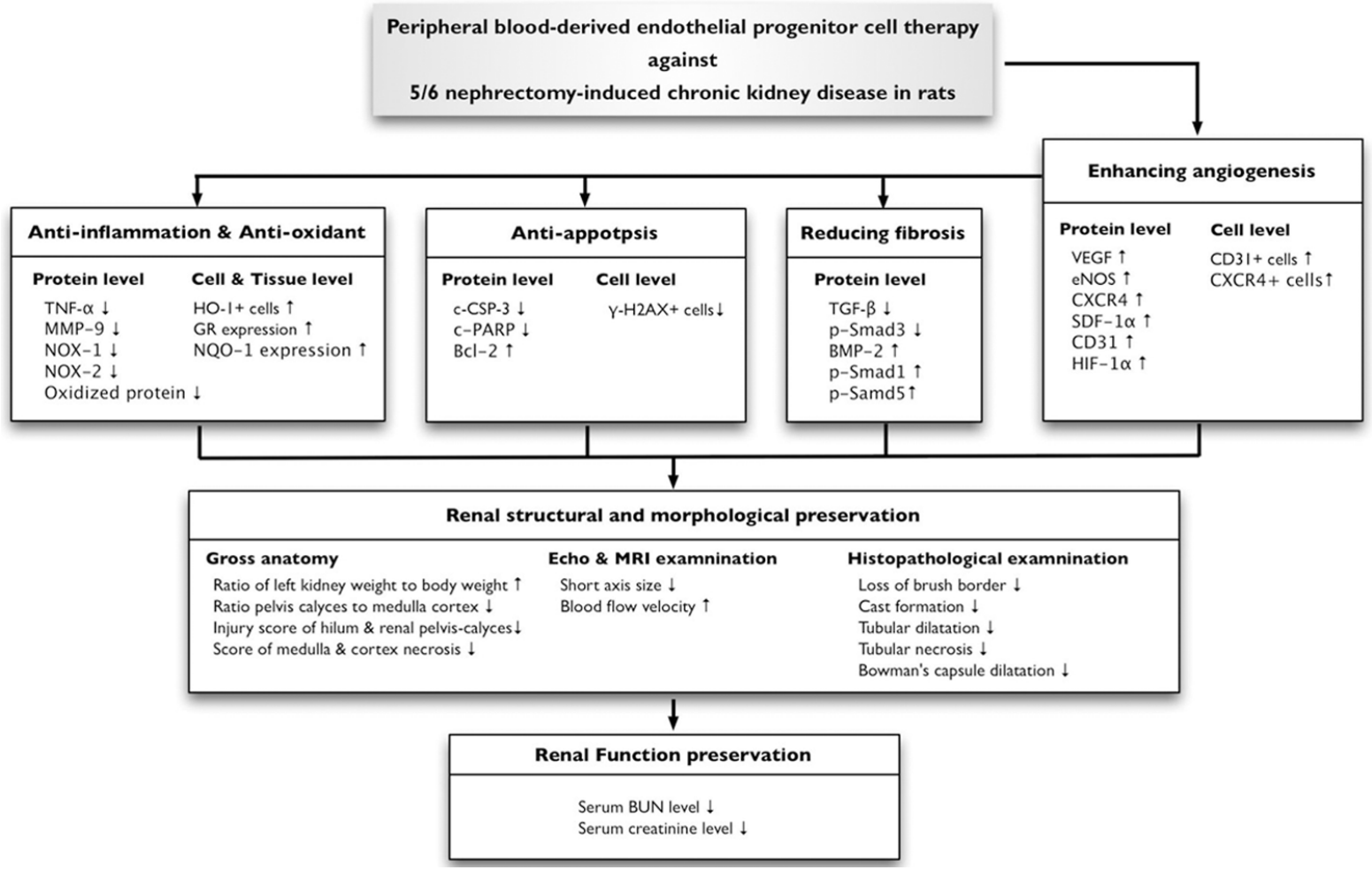

Figure 11. Proposed mechanisms underlying the positive therapeutic effects of peripheral blood-derived endothelial progenitor cells on chronic kidney disease. TNF-α = tumor necrosis factor-α; MMP-9 = matrix metalloproteinase (MMP)-9; HO-1 = heme oxygenase 1; GR = glutathione reductase; NQO 1 = NAD(P)H quinone oxidoreductase; c-CSP-3 = cleaved caspase 3; c-PARP = cleaved poly (ADP-ribose) polymerase; TGF-β = transforming growth factor-β; BMP-2 = bone morphogenetic protein 2; VEGF = vascular endothelial growth factor; eNOS = endothelial nitric oxide synthase; SDF-1α = stromal cell-derived factor-1α; HIF = hypoxic inducible factor; BUN = blood urea nitrogen.

Gung University (Grant number: CMRPG8D-1231) and Ministry of Science and Technology (Grant number: NMRPG8E0021). We thank the molecular imaging core of the Center for Translational Research in Biomedical Sciences, Kaohsiung Chang Gung Memorial Hospital, Kaohsiung, Taiwan for technical and facility supports on Echo Vevo 2100.

Disclosure of conflict of interest

None.

Address correspondence to: Dr. Hon-Kan Yip, Division of Cardiology, Department of Internal Medicine, Kaohsiung Chang Gung Memorial Hospital, 123, Dapi Road, Niaosung Dist., Kaohsiung city, 83301, Taiwan, R.O.C. Tel: +886-7-7317123; Fax: +886-7-7322402; E-mail: han.gung@msa.hinet.net; Cheuk-Kwan Sun, Department of Emergency Medicine, E-DA Hospital, I-Shou University, Kaohsiung, 82445, Taiwan; E-mail: lawrence.c.k.sun@gmail.com

References

[1] Go AS, Chertow GM, Fan D, McCulloch CE and Hsu CY. Chronic kidney disease and the risks of death, cardiovascular events, and hospitalization. N Engl J Med 2004; 351: 1296-1305.

[2] Hsu CC, Hwang SJ, Wen CP, Chang HY, Chen T, Shiu RS, Horng SS, Chang YK and Yang WC. High prevalence and low awareness of CKD in Taiwan: a study on the relationship between serum creatinine and awareness from a nationally representative survey. Am J Kidney Dis 2006; 48: 727-738.

[3] Kuo HW, Tsai SS, Tiao MM and Yang CY. Epidemiological features of CKD in Taiwan. Am J Kidney Dis 2007; 49: 46-55.

[4] Laliberte F, Bookhart BK, Vekeman F, Corral M, Duh MS, Bailey RA, Piech CT and Lefebvre P. Direct all-cause health care costs associated with chronic kidney disease in patients with diabetes and hypertension: a managed care perspective. J Manag Care Pharm 2009; 15: 312-322.

[5] Mende CW. Application of direct renin inhibition to chronic kidney disease. Cardiovasc Drugs Ther 2010; 24: 139-149.

[6] Mogensen CE, Neldam S, Tikkanen I, Oren S, Viskoper R, Watts RW and Cooper ME. Randomised controlled trial of dual blockade of renin-angiotensin system in patients with hypertension, microalbuminuria, and non-insulin dependent diabetes: the candesartan and lisinopril microalbuminuria (CALM) study. BMJ 2000; 321: 1440-1444.

[7] Shroff GR, Solid CA and Herzog CA. Response to letter regarding article, "Long-term survival and repeat coronary revascularization in dialysis patients after surgical and percutaneous coronary revascularization with drug-eluting and bare metal stents in the United States". Circulation 2013; 128: e407.

[8] Viberti G, Wheeldon NM and MicroAlbuminuria Reduction With VSI. Microalbuminuria reduction with valsartan in patients with type 2 diabetes mellitus: a blood pressure-independent effect. Circulation 2002; 106: 672-678.

[9] Al Suwaidi J, Reddan DN, Williams K, Pieper KS, Harrington RA, Califf RM, Granger CB, Ohman EM, Holmes DR Jr; GUSTO-IIb, GUSTO-III, PURSUIT. Global Use of Strategies to Open Occluded Coronary Arteries. Platelet Glycoprotein IIb/IIIa in Unstable Angina: Receptor Suppression Using Integrilin Therapy; PARAGON-A Investigators. Platelet IIb/IIIa Antagonism for the Reduction of Acute coronary syndrome events in a Global Organization Network. Prognostic implications of abnormalities in renal function in patients with acute coronary syndromes. Circulation 2002; 106: 974-980.

[10] Fried LF, Orchard TJ and Kasiske BL. Effect of lipid reduction on the progression of renal disease: a meta-analysis. Kidney Int 2001; 59: 260-269.

[11] Reis SE, Olson MB, Fried L, Reeser V, Mankad S, Pepine CJ, Kerensky R, Merz CN, Sharaf BL, Sopko G, Rogers WJ and Holubkov R. Mild renal insufficiency is associated with angiographic coronary artery disease in women. Circulation 2002; 105: 2826-2829.

[12] Tonelli M, Moye L, Sacks FM, Kiberd B, Curhan G, Cholesterol and Recurrent Events Trial I. Pravastatin for secondary prevention of cardiovascular events in persons with mild chronic renal insufficiency. Ann Intern Med 2003; 138: 98-104.

[13] Basile DP. The transforming growth factor beta system in kidney disease and repair: recent progress and future directions. Curr Opin Nephrol Hypertens 1999; 8: 21-30.

[14] Cybulsky AV. Growth factor pathways in proliferative glomerulonephritis. Curr Opin Nephrol Hypertens 2000; 9: 217-223.

[15] El-Nahas AM. Plasticity of kidney cells: role in kidney remodeling and scarring. Kidney Int 2003; 64: 1553-1563.
[16] Flanders KC. Smad3 as a mediator of the fibrotic response. Int J Exp Pathol 2004; 85: 47-64.
[17] Yang CS, Lin CH, Chang SH and Hsu HC. Rapidly progressive fibrosing interstitial nephritis associated with Chinese herbal drugs. Am J Kidney Dis 2000; 35: 313-318.
[18] Leu S, Sun CK, Sheu JJ, Chang LT, Yuen CM, Yen CH, Chiang CH, Ko SF, Pei SN, Chua S, Youssef AA, Wu CJ and Yip HK. Autologous bone marrow cell implantation attenuates left ventricular remodeling and improves heart function in porcine myocardial infarction: an echocardiographic, six-month angiographic, and molecular-cellular study. Int J Cardiol 2011; 150: 156-168.
[19] Tang XL, Rokosh G, Sanganalmath SK, Yuan F, Sato H, Mu J, Dai S, Li C, Chen N, Peng Y, Dawn B, Hunt G, Leri A, Kajstura J, Tiwari S, Shirk G, Anversa P and Bolli R. Intracoronary administration of cardiac progenitor cells alleviates left ventricular dysfunction in rats with a 30-day-old infarction. Circulation 2010; 121: 293-305.
[20] Wolf D, Reinhard A, Seckinger A, Katus HA, Kuecherer H and Hansen A. Dose-dependent effects of intravenous allogeneic mesenchymal stem cells in the infarcted porcine heart. Stem Cells Dev 2009; 18: 321-329.
[21] Assmus B, Rolf A, Erbs S, Elsässer A, Haberbosch W, Hambrecht R, Tillmanns H, Yu J, Corti R, Mathey DG, Hamm CW, Süselbeck T, Tonn T, Dimmeler S, Dill T, Zeiher AM, Schächinger V; REPAIR-AMI Investigators. Clinical outcome 2 years after intracoronary administration of bone marrow-derived progenitor cells in acute myocardial infarction. Circ Heart Fail 2010; 3: 89-96.
[22] Iwasaki H, Kawamoto A, Ishikawa M, Oyamada A, Nakamori S, Nishimura H, Sadamoto K, Horii M, Matsumoto T, Murasawa S, Shibata T, Suehiro S and Asahara T. Dose-dependent contribution of CD34-positive cell transplantation to concurrent vasculogenesis and cardiomyogenesis for functional regenerative recovery after myocardial infarction. Circulation 2006; 113: 1311-1325.
[23] Kang HJ, Kim HS, Zhang SY, Park KW, Cho HJ, Koo BK, Kim YJ, Soo Lee D, Sohn DW, Han KS, Oh BH, Lee MM and Park YB. Effects of intracoronary infusion of peripheral blood stem-cells mobilised with granulocyte-colony stimulating factor on left ventricular systolic function and restenosis after coronary stenting in myocardial infarction: the MAGIC cell randomised clinical trial. Lancet 2004; 363: 751-756.
[24] Schächinger V, Assmus B, Erbs S, Elsässer A, Haberbosch W, Hambrecht R, Yu J, Corti R, Mathey DG, Hamm CW, Tonn T, Dimmeler S, Zeiher AM; REPAIR-AMI investigators. Intracoronary infusion of bone marrow-derived mononuclear cells abrogates adverse left ventricular remodelling post-acute myocardial infarction: insights from the reinfusion of enriched progenitor cells and infarct remodelling in acute myocardial infarction (REPAIR-AMI) trial. Eur J Heart Fail 2009; 11: 973-979.
[25] Tendera M, Wojakowski W, Ruzyłło W, Chojnowska L, Kepka C, Tracz W, Musiałek P, Piwowarska W, Nessler J, Buszman P, Grajek S, Breborowicz P, Majka M, Ratajczak MZ; REGENT Investigators. Intracoronary infusion of bone marrow-derived selected CD34+CXCR4+ cells and non-selected mononuclear cells in patients with acute STEMI and reduced left ventricular ejection fraction: results of randomized, multicentre Myocardial Regeneration by Intracoronary Infusion of Selected Population of Stem Cells in Acute Myocardial Infarction (REGENT) Trial. Eur Heart J 2009; 30: 1313-1321.
[26] Jie KE, Zaikova MA, Bergevoet MW, Westerweel PE, Rastmanesh M, Blankestijn PJ, Boer WH, Braam B and Verhaar MC. Progenitor cells and vascular function are impaired in patients with chronic kidney disease. Nephrol Dial Transplant 2010; 25: 1875-1882.
[27] Krenning G, Dankers PY, Drouven JW, Waanders F, Franssen CF, van Luyn MJ, Harmsen MC and Popa ER. Endothelial progenitor cell dysfunction in patients with progressive chronic kidney disease. Am J Physiol Renal Physiol 2009; 296: F1314-1322.
[28] Chen YT, Cheng BC, Ko SF, Chen CH, Tsai TH, Leu S, Chang HW, Chung SY, Chua S, Yeh KH, Chen YL and Yip HK. Value and level of circulating endothelial progenitor cells, angiogenesis factors and mononuclear cell apoptosis in patients with chronic kidney disease. Clin Exp Nephrol 2013; 17: 83-91.
[29] Sun CK, Lin YC, Yuen CM, Chua S, Chang LT, Sheu JJ, Lee FY, Fu M, Leu S and Yip HK. Enhanced protection against pulmonary hypertension with sildenafil and endothelial progenitor cell in rats. Int J Cardiol 2012; 162: 45-58.
[30] Yeh KH, Sheu JJ, Lin YC, Sun CK, Chang LT, Kao YH, Yen CH, Shao PL, Tsai TH, Chen YL, Chua S, Leu S and Yip HK. Benefit of combined extracorporeal shock wave and bone marrow-derived endothelial progenitor cells in protection against critical limb ischemia in rats. Crit Care Med 2012; 40: 169-177.
[31] Yip HK, Chang LT, Sun CK, Sheu JJ, Chiang CH, Youssef AA, Lee FY, Wu CJ and Fu M. Autologous transplantation of bone marrow-derived

endothelial progenitor cells attenuates monocrotaline-induced pulmonary arterial hypertension in rats. Crit Care Med 2008; 36: 873-880.
[32] Chen HH, Lin KC, Wallace CG, Chen YT, Yang CC, Leu S, Chen YC, Sun CK, Tsai TH, Chen YL, Chung SY, Chang CL and Yip HK. Additional benefit of combined therapy with melatonin and apoptotic adipose-derived mesenchymal stem cell against sepsis-induced kidney injury. J Pineal Res 2014; 57: 16-32.
[33] Chen YT, Sun CK, Lin YC, Chang LT, Chen YL, Tsai TH, Chung SY, Chua S, Kao YH, Yen CH, Shao PL, Chang KC, Leu S and Yip HK. Adipose-derived mesenchymal stem cell protects kidneys against ischemia-reperfusion injury through suppressing oxidative stress and inflammatory reaction. J Transl Med 2011; 9: 51.
[34] Yip HK, Chang YC, Wallace CG, Chang LT, Tsai TH, Chen YL, Chang HW, Leu S, Zhen YY, Tsai CY, Yeh KH, Sun CK and Yen CH. Melatonin treatment improves adipose-derived mesenchymal stem cell therapy for acute lung ischemia-reperfusion injury. J Pineal Res 2013; 54: 207-221.
[35] Chade AR, Zhu X, Lavi R, Krier JD, Pislaru S, Simari RD, Napoli C, Lerman A and Lerman LO. Endothelial progenitor cells restore renal function in chronic experimental renovascular disease. Circulation 2009; 119: 547-557.
[36] Sangidorj O, Yang SH, Jang HR, Lee JP, Cha RH, Kim SM, Lim CS and Kim YS. Bone marrow-derived endothelial progenitor cells confer renal protection in a murine chronic renal failure model. Am J Physiol Renal Physiol 2010; 299: F325-335.